J Sol-Gel Sci Technol (2017) 82:28–39
DOI 10.1007/s10971-016-4284-9

ORIGINAL PAPER: CHARACTERIZATION METHODS OF SOL-GEL AND HYBRID MATERIALS

Effect of the method and impregnation time on the surface acidity of zirconia modified with boron

María Isabel Arregoitia-Quezada[1] · Ricardo García-Alamilla[1] · Juan Manuel Hernández-Enríquez[1] · Francisco Paraguay-Delgado[2] · Luz Arcelia Garcia-Serrano[3] · José Luis Rivera-Armenta[1]

Received: 5 June 2016 / Accepted: 9 December 2016 / Published online: 30 December 2016

Abstract In this paper, the synthesis and characterization of boron-modified zirconia is reported. The zirconium hydroxide obtained by sol-gel was modified with boric acid, in order to increase the surface acidity of the zirconia. For this purpose, two impregnation methods were used: conventional and ultrasonic, and the impregnation time was set at 1 or 4 h. The synthesized materials were characterized by thermal analyses, X-ray diffraction, infrared spectroscopy, nitrogen physisorption, and scanning electron microscopy. The boron incorporation delayed the crystallization of solids, which were mainly amorphous but with tendency toward the formation of the tetragonal phase. The modified materials were micro-mesoporous and their specific area was improved, while the pure zirconia showed a lower nitrogen adsorption. Units BO_3 and BO_4 were identified, confirming the boron presence. In general, the solids showed spherical particles; however, the ultrasonic treatment originated elongated particles. In addition, the acidic properties were evaluated by potentiometric titration and ethanol decomposition. The maximum acid strength of the zirconia increased from −28 mV to over 200 mV; consequently, all the boron-modified materials showed strong and very strong acid sites. The influence on the catalytic activity, due to the method and impregnation time, was clearly observed in the ethanol decomposition. The most active catalysts were those obtained by the ultrasonic method and the best was that impregnated during 1 h.

Graphical Abstract

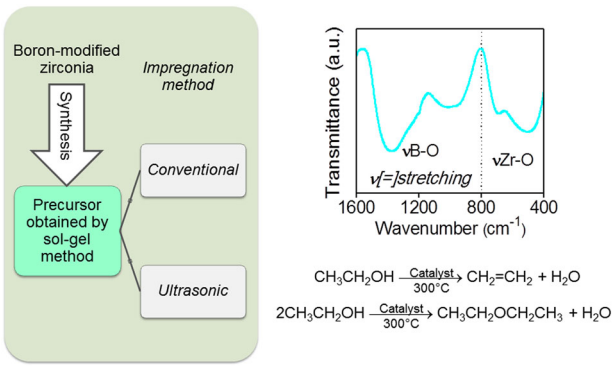

Keywords Zirconia · Boron · Sol-gel · Ultrasound · Surface acidity

✉ Ricardo García-Alamilla
ricardogarcia.alamilla@yahoo.com.mx

[1] Centro de Investigación en Petroquímica Secundaria del Instituto Tecnológico de Ciudad Madero (CIPS-ITCM), Prolongación Bahía de Adair, Av. de las Bahías, Parque de la Pequeña y Mediana Industria, Altamira, Tamaulipas, México

[2] Centro de Investigación en Materiales Avanzados (CIMAV), Av. Miguel de Cervantes 120, 31109 Chihuahua, Chihuahua, México

[3] Centro Interdisciplinario de Investigaciones y Estudios sobre Medio Ambiente y Desarrollo del Instituto Politécnico Nacional (CIIEMAD-IPN), 30 de Junio de 1520 S/N, Barrio La Laguna Ticomán, Cd. de México, Distrito Federal, México

1 Introduction

In the field of heterogeneous catalysis, the aim of several studies has been the development of solid catalysts with acidic properties, and metal oxides have been the basis of numerous research works. In this context, zirconium oxide or zirconia (ZrO_2) is notable for its high thermal stability, as well as for its redox and acid–base properties. Furthermore,

the addition of oxoanions (SO_4^{2-}, WO_4^{2-}, and MoO_4^{2-}) leads to increase in its acid strength [1]. Sulfated zirconia (SO_4^{2-}/ZrO_2) has strong acid sites and crystalline properties that allow it to catalyze the isomerization of light paraffins and other reactions promoted by acidity [2–5]. The preparation method selected as well as the synthesis variables involved have a marked influence on the catalytic activity of sulfated zirconia, and this has generated abundant literature about the effect of different preparation parameters on the final properties of this material [5–8]. Sulfuric acid is used as sulfating agent to obtain SO_4^{2-}/ZrO_2; nevertheless, the modification of zirconia with other mineral acids (phosphoric or boric) produces materials with acidic properties suitable for catalytic applications, although these have lower acid strength compared to its sulfated counterpart [9–11]. On this matter, we can refer to the modification of ZrO_2 with boric acid in aqueous solution, using the incipient wetness technique. It should be noted that the support was previously calcined at 500 °C, and it was heat-treated at 350 °C after impregnation. This catalyst was highly active and selective for the synthesis of ε-caprolactam, being superior in comparison to other supports treated with boric acid (Al_2O_3, TiO_2, SiO_2, MgO, and HZSM-5) [12]. In a later work, these researchers suggested that a better method for the preparation of the catalyst may be a direct modification of the hydroxide precursor with boric acid, followed by calcination at a temperature as high as 600 °C [13]. Afterwards, some researchers have generally obtained catalysts from an amorphous precursor of zirconia, impregnated with an aqueous solution of boric acid and, subsequently, heat-treated at different temperatures. Boron-modified zirconia (B_2O_3/ZrO_2) is active in various industrially important organic transformations such as benzoylation of anisole [10], methylation of phenol [14], transesterification of β-ketoesters [15], and condensation of Knoevenagel [16, 17], among others. In those studies, hydroxide precursor was prepared from zirconium salt precipitation; the powder obtained was added to an aqueous solution of boric acid, stirring constantly until slurry was obtained. The calcination temperature of the solid, obtained after drying, was within the range of 500–750 °C [10, 14–16]. On the other hand, the synthesis of support by micellar method was reported, varying the zirconium concentration in the starting solution, as well as the boron concentration in the solution used for impregnation. In contrast to the above-mentioned studies, these catalysts were calcined at a relatively low temperature (320 °C); however, they showed activity in the acetylation of 2-phenoxyethanol [18].

In particular, we considered it feasible to continue exploring the influence of different synthesis parameters on the physicochemical properties of boron-modified zirconia. According to literature, ultrasonic waves can enhance and promote the active species dispersion on the support surface, thereby improving the catalyst performance [19, 20]. Therefore, the aim of this work is to compare and discern whether there are differences between the materials prepared by conventional impregnation and those obtained by ultrasonic impregnation, applying the vibration generated in an ultrasound bath.

2 Experimental

2.1 Chemicals

Zirconium(IV) butoxide solution ($Zr[O(CH_2)_3CH_3]_4$; 80 wt% in 1-butanol, Sigma-Aldrich), 1-butanol ($CH_3(CH_2)_3OH$; 99.8% anhydrous, Sigma-Aldrich), distilled water (Quimicrón), and boric acid (H_3BO_3, 99.5%, Técnica Química) were used for the preparation of the catalysts.

2.2 Synthesis

Zirconium hydroxide was prepared via sol-gel using molar ratios established in alcohol/alkoxide = 12 and water/alkoxide = 8. Zirconium(IV) butoxide was dissolved in 1-butanol by constant stirring at 70 °C. The homogenized solution was hydrolyzed by slow drip with distilled water and the gel produced was aged 72 h at room temperature. Subsequently, the excess of solvent was evaporated at 100 °C in a muffle furnace. The powder obtained was added to an aqueous solution of boric acid to deposit 3.7% theoretical weight of boron on the support, and this suspension was stirred for 1 or 4 h. Similarly, the impregnation was performed using the vibration generated in an ultrasound bath Crest Ultrasonics model CP1200D (45 kHz, sonic power: step 3). The modified zirconium hydroxides were dried at 110 °C, and then they were calcined for 3 h at 600 °C, at a heating rate of 5 °C/min under air dynamic atmosphere. The nomenclature identifies the synthesized catalysts according to the method (C = conventional or U = ultrasonic) and impregnation time: ZB1hC, ZB4hC, ZB1hU, and ZB4hU. In addition, a portion of unmodified zirconium hydroxide was calcined in the same way to obtain the pure zirconia, ZrO_2.

2.3 Characterization

Precursors of materials (zirconium hydroxides: pure and boron-modified) were thermally analyzed in airflow (30 mL/min) at a heating rate of 5 °C/min from room temperature to 900 °C (TA Instruments SDT 2960 Simultaneous DSC-TGA). The X-ray diffraction (XRD) patterns of the oxides were obtained in the 2 θ angular range from 20 to 80°, using Cu Kα radiation ($\lambda = 0.15406$ nm) and a scanning rate of 0.2 rad/s (Bruker D8 Advanced). Infrared

spectra were collected using pellets of the sample in KBr, and the measurements were performed in the range of 400–4000 cm^{-1} with 16 scans and a resolution of 4 cm^{-1} (Perkin Elmer Spectrum 100). The textural properties of the solids were determined from the adsorption-desorption isotherms of nitrogen; the samples were degassed previously at 250 °C (Quantachrome Autosorb-1). The surface morphology of the materials was observed by means of electronic images obtained using a scanning microscope with an accelerating voltage of 2.0 kV (Jeol JSM 5800LV). The acidic properties were evaluated by the potentiometric titration technique with *n*-butylamine and by the ethanol decomposition reaction. After 3 h of constant stirring, the solid suspended in acetonitrile was titrated using a solution of *n*-butylamine 0.025 N and the variation of the electrode potential was recorded until the equilibrium was reached (Chemcadet Cole Parmer). The ethanol decomposition was carried out at 300 °C with 100 mg of catalyst placed in a fixed-bed tubular reactor. The microplant of catalytic activity operates at atmospheric pressure and continuous flow. The reaction products were analyzed on-line by a gas chromatograph (Varian 3400 FID).

3 Results and discussion

3.1 Thermal analysis (DTA-TGA)

The thermal behavior of the synthesized hydroxides is shown in Figs. 1 and 2, analyzing from room temperature to 900 °C. Boron-modified solids showed less weight loss compared to their pure counterpart, consequence of the boron presence. All DTA profiles presented a similar behavior at low temperature (50–100 °C), which corresponds to the removal of physically adsorbed moisture [18, 21]. After that endothermic process, in the range of 100–900 °C, the modified materials had similar percentages of weight loss: 10.8, 10.9, 10.1, and 10.0, respectively, for the final oxides ZB1hC, ZB4hC, ZB1hU, and ZB4hU. Therefore, the observed differences in the values of total weight loss are not related to time or impregnation method, rather it is a result of the moisture present in each sample. Melada et al. [6] analyzed TGA profiles of sulfated zirconia xerogels and indicated that the weight loss recorded in the 150–350 °C range was due to dehydration and dehydroxylation processes, as well as the elimination of carbonaceous species from the surface. Accordingly, the maximums located at 269 and 303 °C in the DTA curve of pure precursor (Fig. 2) are attributed to the combustion of residual organic groups, since the zirconium hydroxide was obtained from the hydrolysis of an alkoxide [6, 21]. Precursors of the boron-modified oxides did not present those peaks, but they exhibited a gradual weight loss in the range of 100–500 °C (Fig. 1), which would include the changes reported by Melada et al. [6]. Finally, the exothermic signal observed at 405 °C is assigned to the transformation of an amorphous state to a crystalline zirconia [18, 21]; nevertheless, this change occurred at a higher temperature (682–685 °C) by effect of the addition of boron, so it follows that the boron presence retards the crystallization process of the material. Ivanov et al. [22] observed similar behavior due to the introduction of sulfate ions, which favors the stabilization of the amorphous zirconia and delays the crystallization process. For their part, Osiglio et al. [18] indicated that the crystallization of zirconia, obtained by the micellar method, showed a maximum at 440 °C in the DTA diagram; however, this signal was presented with peaks at 630, 732, and 697 °C, depending on the content boron in the samples. The materials analyzed in this study were modified with the same theoretical content of boron (3.7 wt%); thus, the signal

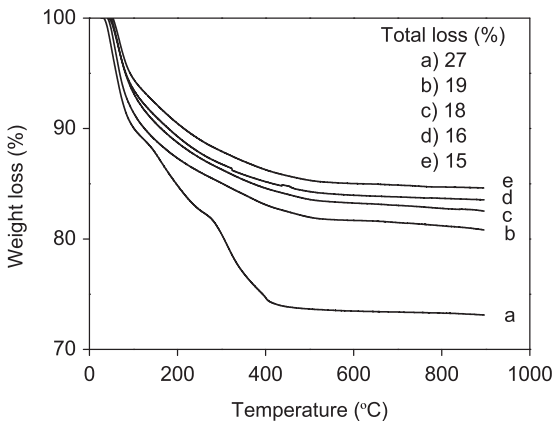

Fig. 1 TGA profiles of the catalytic precursors (zirconium hydroxides: pure and boron-modified): **a** pure, **b** HB1hC, **c** HB4hC, **d** HB1hU, and **e** HB4hU

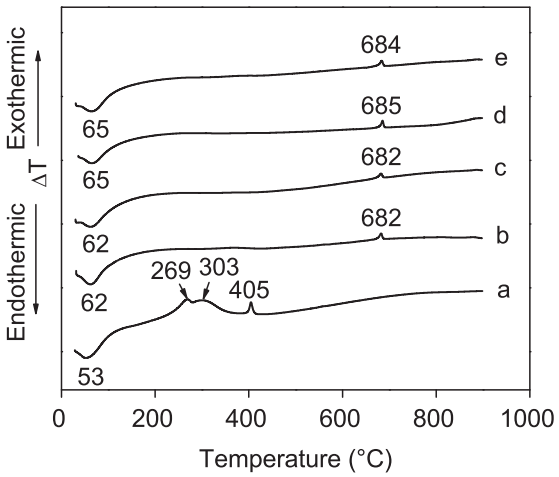

Fig. 2 DTA profiles of the catalytic precursors (zirconium hydroxides: pure and boron-modified): **a** pure, **b** HB1hC, **c** HB4hC, **d** HB1hU, and **e** HB4hU

position attributed to the crystallization is practically the same for all solids, indistinctly of the method or impregnation time. Above 500 °C, there were no significant weight changes in the TGA profiles of the modified materials; hence, it is important to note that there is no evidence of boron species evacuation. This last observation allows us to infer a strong interaction between the boron and zirconia framework, and may represent a convenient feature compared to its sulfated counterpart. It is well known, in the particular case of sulfated zirconia xerogels, that sulfate ions begin to decompose at temperatures above 600 °C, generating both an endothermic signal in the DTA profile and a marked weight loss in the TGA curve [6, 22]. Moreover, the loss of sulfate groups also occurs above 600 °C even in sulfated zirconia previously calcined [2], which is a disadvantage for regeneration processes at high temperatures. Conversely, boric acid was thermally analyzed under the same conditions as the catalytic precursors. The endothermic changes at 118 and 161 °C are associated with the dehydration of boric acid (DTA profile not shown), thereby generating the formation of boron oxide (B_2O_3) [23, 24].

3.2 X-ray diffraction

The XRD pattern of ZrO_2 powder calcined at 600 °C (Fig. 3) mainly presented diffraction lines assigned to the tetragonal phase at $2\theta = 30.210°$, 34.570°, 35.248°, 42.966°, 50.201°, 50.705°, 59.266°, 60.165°, 62.823°, 72.919°, and 74.536° (PDF 01-072-7115). The presence of the monoclinic phase was identified in low proportion, showing very weak signals at $2\theta = 28.182°$ and 31.472° (PDF 01-081-1314). In accordance with the DTA profile corresponding to the precursor ZrO_2 (shown in Fig. 2), the transition from amorphous phase to a crystalline structure occurs at 405 °C; therefore, heating at 600 °C generated well-crystallized zirconia. On the other hand, the XRD patterns of the modified solids (Fig. 4) confirmed the delay in the crystallization of these materials due to the boron incorporation, also according to the DTA curves (Fig. 2)

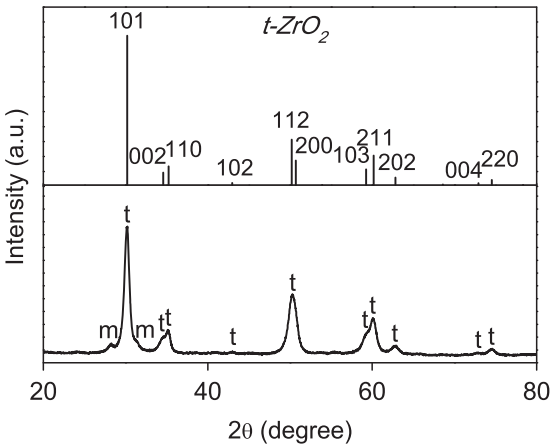

Fig. 3 XRD pattern of the material ZrO_2

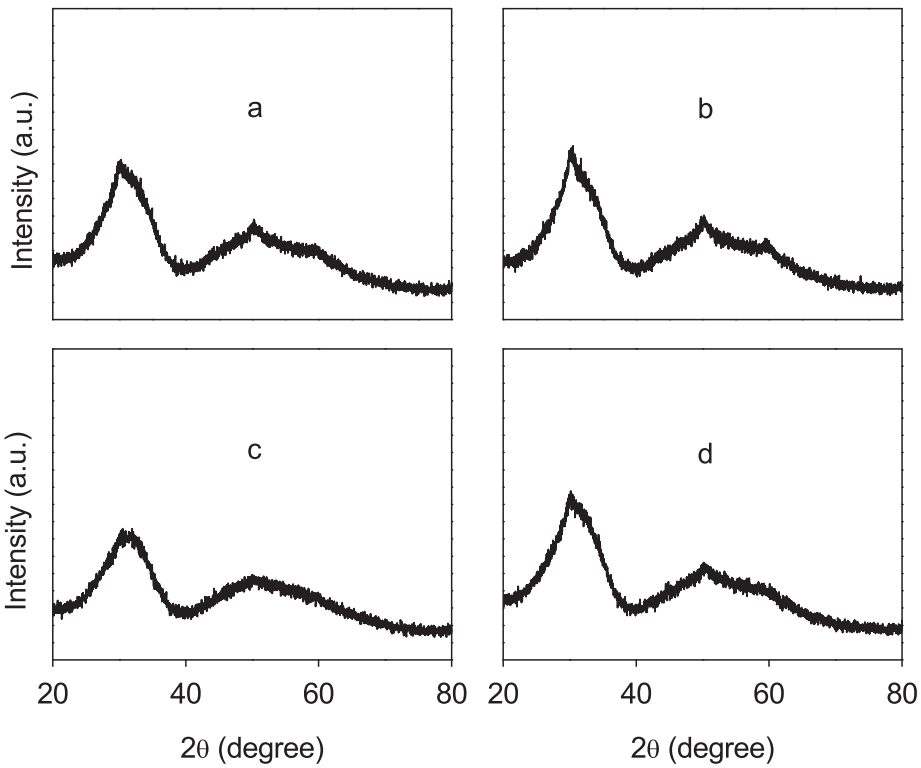

Fig. 4 XRD patterns of modified materials: **a** ZB1hC, **b** ZB4hC, **c** ZB1hU, and **d** ZB4hU

that exhibited this structural change with a maximum around 680 °C. The intensity of the diffraction signals decreased significantly, showing an amorphous tendency; however, the broad peak centered on 30° in 2θ scale suggests the formation of an incipient crystalline phase (tetragonal). Conversely, Zaleska et al. [25] synthesized titanium dioxide (TiO_2) of anatase phase, using the sol-gel method, and they reported similar behavior. The addition of H_3BO_3 inhibited crystallite growth and transformation from the amorphous state to the anatase structure. The XRD pattern of TiO_2 with 0.5 wt% of boron presented only a very weak signal attributed to the anatase phase, and the material was amorphous when the boron content increased to 10 wt% [25]. In this work, in order to identify the presence of diffraction signals corresponding to boron oxide in the modified materials, a sample of boric acid was calcined at 600 °C and then it was analyzed by XRD. As noted above, B_2O_3 is formed from the dehydration of H_3BO_3. In the XRD pattern of the boron oxide (not shown) a narrow and intense peak at $2\theta = 27.6°$ was observed [26]. It is important to note that this signal is not seen in the diffractograms of the modified solids (Fig. 4), either due to good dispersion of B_2O_3 in amorphous state or because the crystallites are so small that they cannot be detected by this technique [18].

3.3 Infrared spectroscopy (FT-IR)

The infrared spectrum of the solid ZrO_2 is shown in Fig. 5. In the region assigned to the stretching frequency of O–H bonds (3800–3000 cm^{-1}) only a minuscule signal centered at 3400 cm^{-1} was presented; this slightly pronounced band indicates the removal of surface water because of the high calcination temperature [27, 28]. Moreover, the spectrum also showed an intense band in the region of 800–400 cm^{-1}, with signals around 580 and 495 cm^{-1} that characterize the crystalline zirconia, agreeing with thermal analysis and XRD [27]. The spectra of the boron-modified oxides exhibited the same signals, indistinctly of the method or impregnation time (Fig. 6). The bands observed in the region of 1500–900 cm^{-1} corroborated the presence of boron, since they are attributed to stretching of B–O bonds [29]. Boron may be present in two structural units: trigonal and tetrahedral. The minimums accentuated around 1370 and 1010 cm^{-1}, respectively, correspond to BO_3 and BO_4 species [30]. Furthermore, because of the interaction of boron with zirconia, the band assigned to stretching Zr–O bonds showed a shift of the signals to 685 and 505 cm^{-1}. These spectra also presented a signal at 1630 cm^{-1}, which is attributed to bending vibrations of -(H–O–H)- bonds [27, 28] and a band with minimums in the region of 3400–3200 cm^{-1}, due to stretching of O–H bonds. On the other hand, once thermal analysis was completed (from room temperature to 900 °C), the remaining materials were analyzed

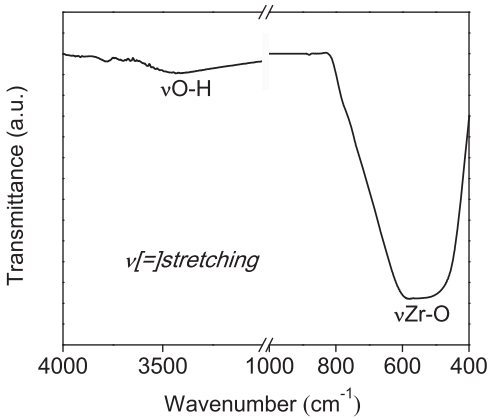

Fig. 5 FT-IR spectrum of the material ZrO_2

by infrared spectroscopy. In Fig. 7, the similarity between the spectra of the samples ZB1hC-R and ZB1hU-R and the spectrum of boric acid can be seen, where absorptions close to 1460 and 1190 cm^{-1} represent BO_3 units [12]. This reveals that the boron species are present in the synthesized materials even at high temperatures of heat treatment.

3.4 Textural properties (N_2 physisorption)

In this work, the boron incorporation promoted an increase in the specific area of the materials in comparison to the pure ZrO_2, reported in Table 1; therefore, boron had a stabilizing effect that prevented the oxides sintering during the calcination step. In correlation to the XRD analysis, only the pure material developed a well-crystallized tetragonal phase, while the modified solids had a lower degree of crystallinity (being mainly amorphous); thus, it is consistent that the materials ZB1hC, ZB4hC, ZB1hU, and ZB4hU have specific area values of the order of 130–170 m^2/g. In general, the solids showed similar textural properties, independently of the method or modification time with boric acid. ZrO_2 presented a type III isotherm (Fig. 8), which is convex toward the abscissa axis for the whole range of relative pressure [27]. This type of isotherm is characteristic of nonporous solids, or possibly macroporous, that have a low energy of adsorption. This is according to the low volume of nitrogen adsorbed by this material. Conversely, the nitrogen physisorption analysis performed to samples of the modified solids revealed isotherms of hybrid form of type I-IV with a narrow hysteresis, appreciable in the materials ZB1hU and ZB4hU (Fig. 9), that indicates the existence of a combination of micro-mesoporosity, confirmed by the pore size distribution (Fig. 10). Sinhamahapatra et al. [31, 32] observed similar behavior in the isotherms of adsorption-desorption of N_2 developed by sulfated and borated zirconia samples, showing average pore size distributions located in the mesoporous region, but

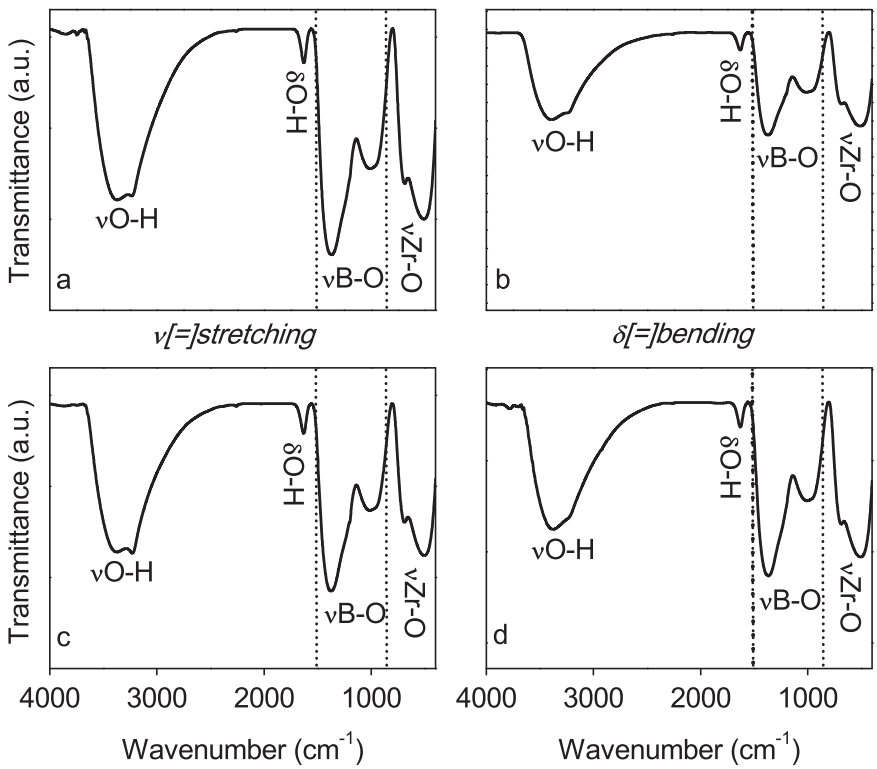

Fig. 6 FT-IR spectra of the modified materials: **a** ZB1hC, **b** ZB4hC, **c** ZB1hU, and **d** ZB4hU

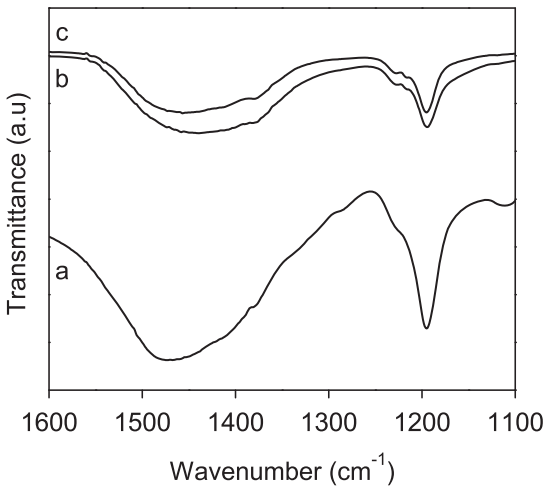

Fig. 7 FT-IR spectra of **a** H_3BO_3 and recovered materials after the thermal analysis: **b** ZB1hU-R and **c** ZB1hC-R

on the border with the microporous region (2–2.7 nm). Similarly, Osiglio et al. [18] obtained borated zirconia catalysts with pores in a like range.

3.5 Scanning electron microscopy (SEM)

The images in Fig. 11 exhibit the morphology of zirconia samples, pure and boron-modified. ZrO_2 showed spherical particles with heterogeneous size (up to 1 μ) and tendency to aggregate formation. The micrographs of the material ZB1hC also showed particles with similar morphology, conserving spherical tendency, and formation of agglomerates; the particle size is in a range of 0.5–1 μ and there are also small aggregates of particles on the surface of the consolidated aggregates. Finally, the images corresponding to the ultrasonically modified material (ZB1hU) showed similarity to the material ZB1hC, although agglomerates were losing their spheroidal shape becoming elongated particles (up to 1 μ); in addition, the growth of particles finer than those observed in the material ZB1hC was noted.

3.6 Acidic properties

3.6.1 Potentiometric titration with n*-butylamine*

The surface acidity of the synthesized materials was determined by potentiometric titration with *n*-butylamine solution in acetonitrile. The basis of this technique establishes that the acid environment around the electrode membrane causes the potential difference; therefore, the measured potential is an indicator of the acidic properties of the dispersed solid particles. The criterion adopted for the interpretation of the results indicates that the maximum acid strength (MAS) of the sites is determined by the initial potential of the electrode (Ei). The acid strength of these sites is classified according to the following scale: $E > 100$ mV

Table 1 Textural and acidic properties of the synthesized materials

Material	S_{BET} (m^2/g)[a]	V_T (cm^3/g)[b]	MAS (mV)	Total acidity (meq n-BTA/g)
ZrO_2	5	0.04	−28	0.28
ZB1hC	168	0.15	244	0.52
ZB4hC	166	0.14	237	0.52
ZB1hU	134	0.15	277	0.62
ZB4hU	168	0.17	225	0.45

[a] Calculated using the Brunauer–Emmett–Teller method, relative pressure range 0.05–0.30

[b] Total pore volume measured near the saturation pressure ($P/P_0 \cong 1$)

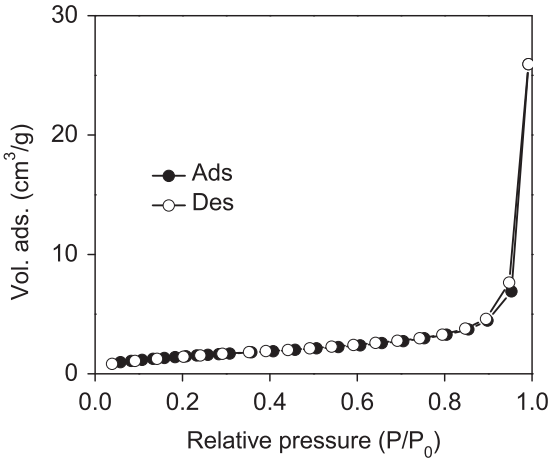

Fig. 8 N_2 adsorption-desorption isotherm of the material ZrO_2

(very strong sites), $0 < E < 100$ mV (strong sites), $-100 < E < 0$ mV (weak sites), and $E < -100$ mV (very weak sites) [33, 34]. In addition, the total number of acid sites corresponds to the value of meq amine/g of solid, which is determined when there are no more changes in the potential. Table 1 shows that all MAS values of the boron-modified samples were > 200 mV in the following order: ZB1hU > ZB1hC > ZB4hC > ZB4hU, while the ZrO_2 only reached −28 mV. The total number of *n*-butylamine milliequivalents, required for neutralization, also confirmed a higher concentration of acid sites in these materials compared to its pure counterpart. Figure 12 presents the titration curves for each solid. ZrO_2 exhibited only weak acid sites, while the impregnation of the catalytic precursors using boric acid generated strong and very strong acid sites in all samples. Neutralization profiles of the catalysts ZB1hC and ZB4hC had similar behavior for potential values > 50 mV (Fig. 12a). The curve of the sample ZB1hC showed stability at values close to 0 mV, so it indicates that this material presented only strong and very strong acid sites, while the material ZB4hC furthermore showed weak sites. On the other hand, Fig. 12b exhibits the neutralization profiles obtained for the samples ZB1hU and ZB4hU, which showed a similar tendency with a distribution of acid sites from very strong to weak. However, between these two materials it is evident that the catalyst ZB1hU encompasses a greater total concentration of acid sites, being even superior to its modified counterpart (ZB1hC).

3.6.2 Ethanol decomposition

Alcohols decomposition is commonly used to study the acid/basic nature of the surface of metal oxides; the formation of aldehydes and ketones occurs via dehydrogenation on basic catalysts, while alcohol dehydration leads to olefins and ethers when acid sites are present [35]. In particular, the products of the ethanol dehydration are ethylene (intramolecular reaction) and diethyl ether (intermolecular reaction) [36–39]. The ethanol decomposition results, conducted at 300 °C, are presented in Fig. 13. In all cases, dehydration products were obtained (Fig. 14), confirming the predominantly acid nature of the synthesized solids. When the reaction was carried out using ZrO_2, 2% conversion was achieved, but a remarkable increase was observed when the boron-modified materials were evaluated. For example, with the solids ZB1hC and ZB4hC, the ethanol conversion increased more than 30 times, oscillating in the range of 60–70%. Conversely, the materials ZB1hU and ZB4hU had a better performance in reaction, obtaining up to 100% of conversion with the catalyst that was ultrasonically modified for 1 h. The latter is consistent with the results of potentiometric titration, since the most active solid has a higher concentration of acid sites and superior MAS. However, it should be noted that the catalyst ZB4hU presented conversions between 70 and 80%, although it was slightly less acidic than the solids ZB1hC and ZB4hC. Therefore, it is possible to suggest a synergistic effect between boron incorporation and its dispersion on the support influenced by the impregnation method, thereby leading to more active catalysts compared to those modified by a conventional method. Moreover, as previously mentioned, all catalysts favored the alcohol decomposition via dehydration, due to an increment in acid strength of the materials by the presence of boron. Even ZrO_2 was selective only to ethylene obtention; nevertheless, its weak acidity led to a very low conversion level. Furthermore, the distribution of the reaction products also indicates influence due to the impregnation method. The

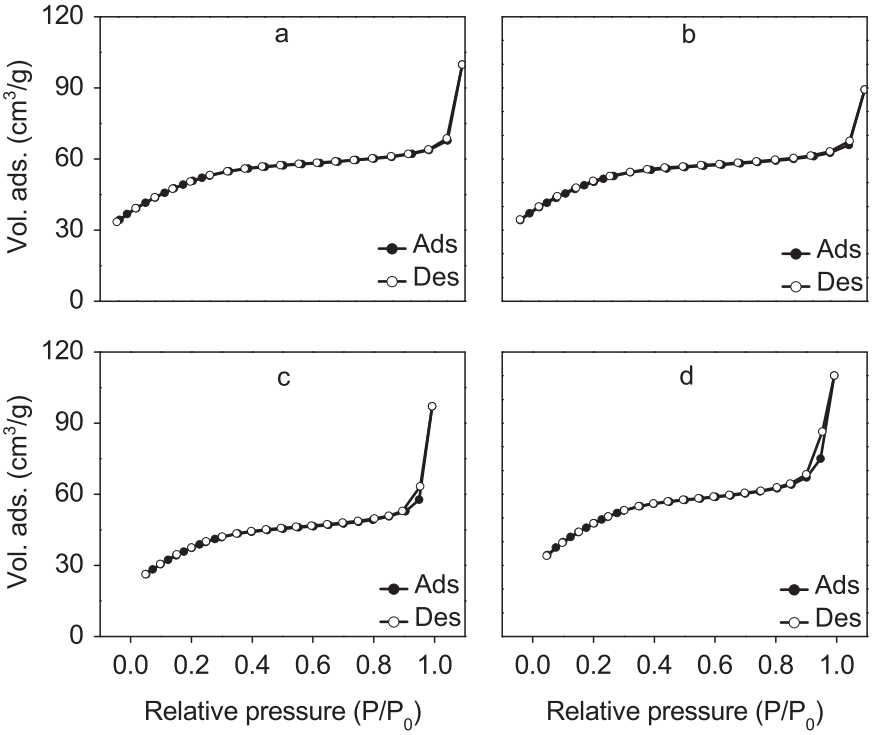

Fig. 9 N_2 adsorption-desorption isotherms of the modified materials: **a** ZB1hC, **b** ZB4hC, **c** ZB1hU, and **d** ZB4hU

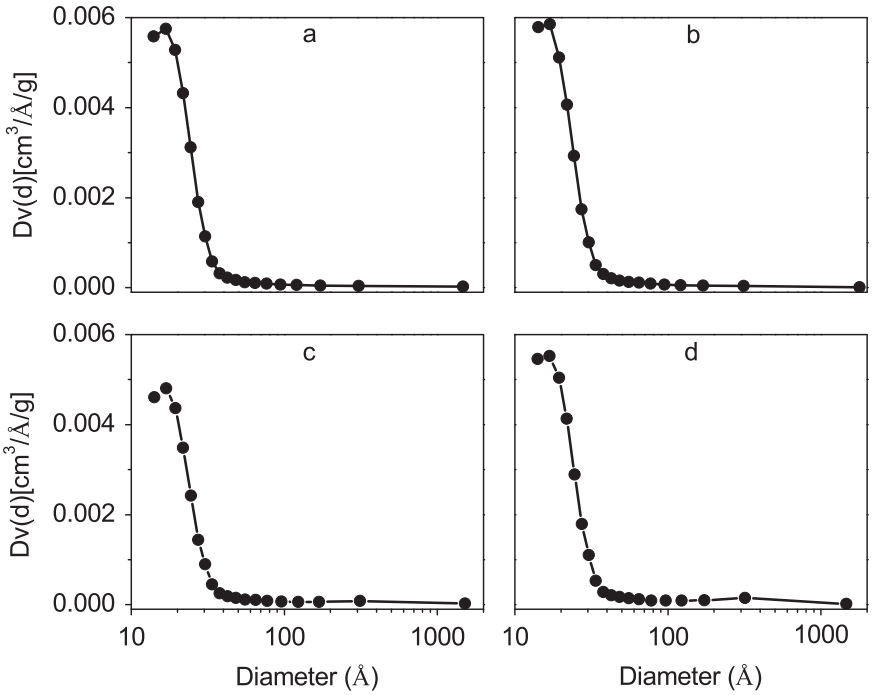

Fig. 10 Pore size distributions of the modified materials: **a** ZB1hC, **b** ZB4hC, **c** ZB1hU, and **d** ZB4hU, estimated by the method of Barret–Joyner–Halenda from the desorption branch

catalysts ZB1hC and ZB4hC were preferably selective to the formation of diethyl ether (60–70%), while the solids ZB1hU and ZB4hU increased the generation of ethylene. In fact, it can be noted that the products distribution is inverse for the catalysts impregnated during 1 h, suggesting that the surface of the solids favors either an elimination mechanism to produce the olefin (ZB1hU) or a substitution mechanism that leads to the formation of ether (ZB1hC).

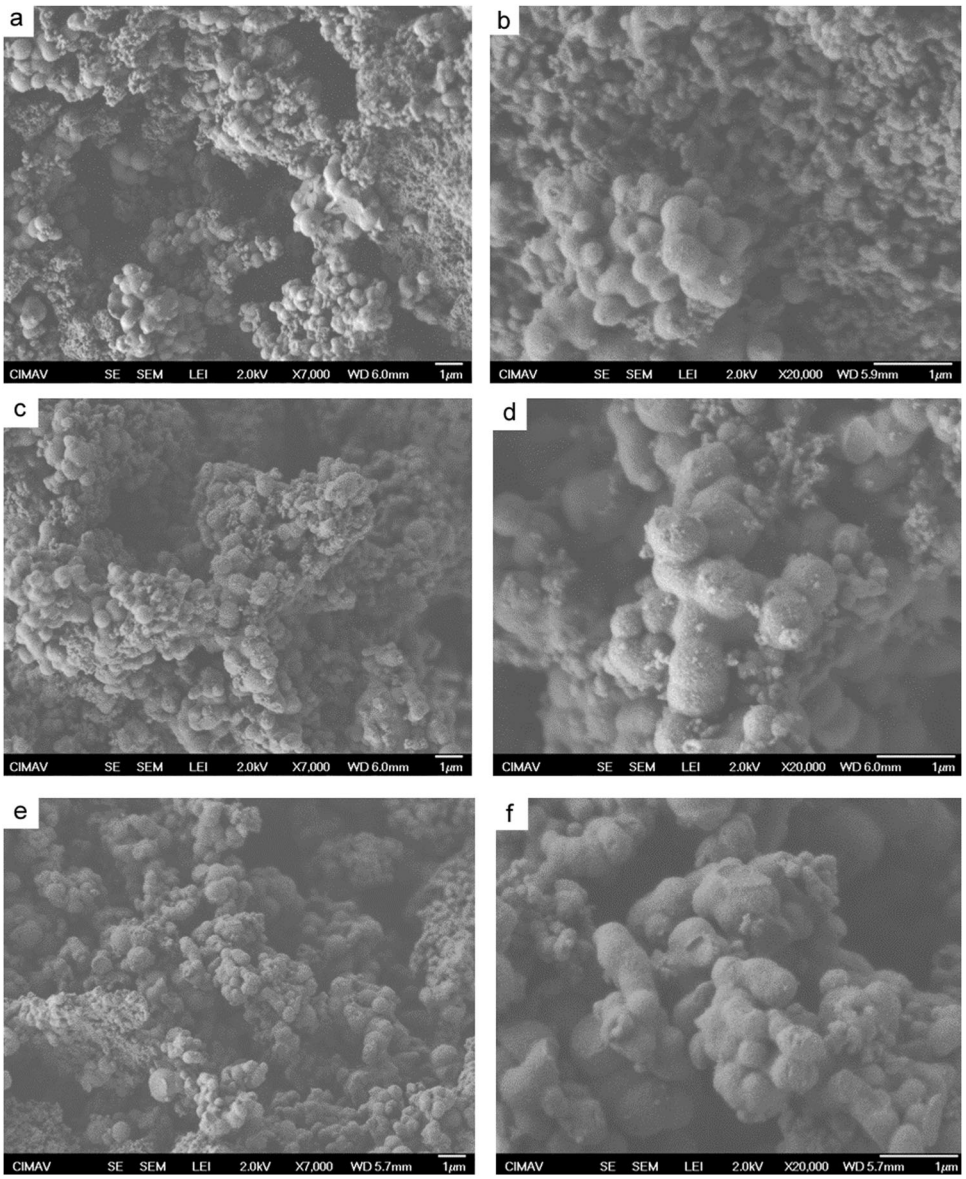

Fig. 11 SEM images of the materials: **a**, **b** ZrO_2, **c**, **d** ZB1hC and **e**, **f** ZB1hU

In Scheme 1 is shown a simplified representation of the ethanol dehydration. Elimination reactions (olefin formation) and substitution reactions (ether formation) are carried out simultaneously and compete with each other. These reactions are superficial and require different types of active sites: acid (electrophilic) and basic (nucleophilic). In general, the alcohol chemisorption on the acid site polarizes the C–O bond, converting the hydroxyl into a better leaving group. Moreover, the alcohol chemisorption on a basic site increases the oxygen nucleophilic character of this molecule. This may cause a nucleophilic displacement on the carbon atom of the adsorbed alcohol on the acid site, which results in the formation of the ether. In an alternative pathway, the adsorbed alcohol molecule on the acid site may lose a β proton to form the olefin [40]. In the literature, it is suggested that dehydration of ethanol to ethylene occurs through a concerted elimination mechanism, E2, involving an acid site and a basic site [41].

A desired feature in solid acid catalysts is their reuse in reaction. The literature regarding the recyclability of boron-modified zirconia is scarce, and such studies involve the use of this catalyst in reactions carried out in liquid phase and at low temperatures (90–150 °C). In general, after at least three reaction cycles, only a slight decrease in the yield of the desired product was observed in the reactions of benzoylation of anisole [10], transesterification of *β*-ketoesters [15], condensation of Knoevenagel [16], and acetylation of 2-phenoxyethanol [18]. Therefore, in our work we decided to test the reusability of the catalyst ZB1hU, which showed a better performance in the ethanol decomposition. The results are presented in Fig. 15. In this case, the reaction was conducted at 250 °C, so it was also possible to observe changes in

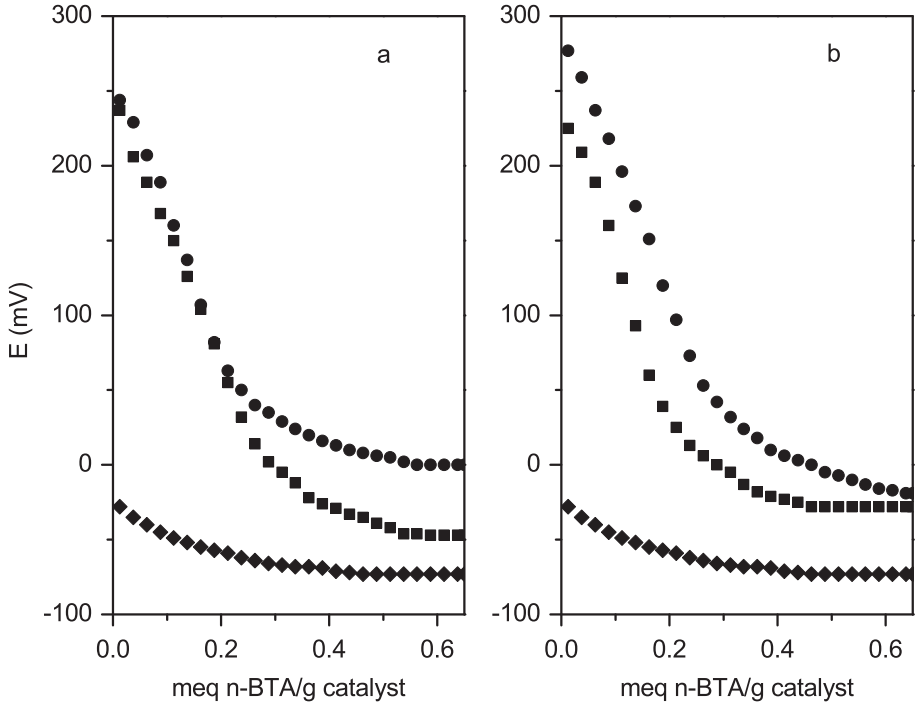

Fig. 12 Potentiometric titration curves for synthesized catalysts: *Black Diamond Suit* ZrO_2, **a** *Black Circle* ZB1hC and *Black Square* ZB4hC, **b** *Black Circle* ZB1hU and *Black Square* ZB4hU. *E* is the electrode potential (mV)

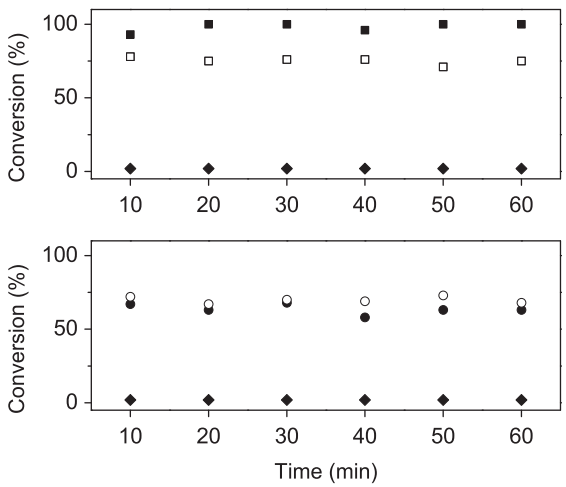

Fig. 13 Ethanol conversion at 300 °C using the synthesized catalysts: *Black Diamond Suit* ZrO_2, *Black Circle* ZB1hC, *White Circle* ZB4hC, *Black Square* ZB1hU, and *White Square* ZB4hU

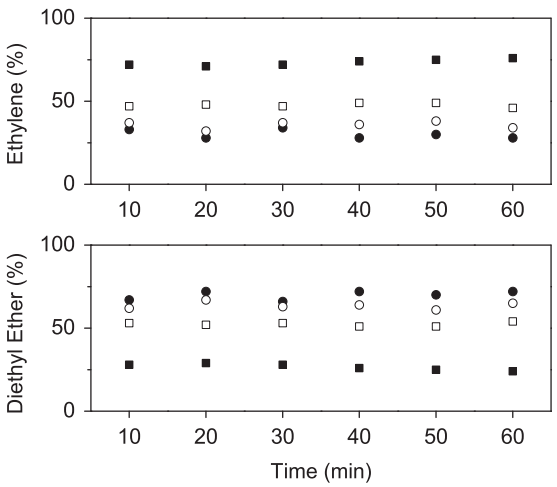

Fig. 14 Products distribution of ethanol dehydration at 300 °C using the synthesized catalysts: *Black Circle* ZB1hC, *White Circle* ZB4hC, *Black Square* ZB1hU, and *White Square* ZB4hU

the products distribution. The conversion was stable around 28%, both with fresh catalyst and with the used material. On the other hand, the selectivity was mainly oriented toward the formation of diethyl ether, as a consequence of a lower reaction temperature compared to the results shown in Fig. 14. It is well known that low temperatures favor the ether obtention, and when the reaction temperature increases the production of the olefin also increases [36–39]. As shown in Fig. 15, the products distribution did not exhibit significant changes when the catalyst was reused. It should be noted that, after finishing the first test, the material was exposed to heat treatment at 270 °C in the presence of a nitrogen stream to evacuate moisture and any impurities.

4 Conclusions

By means of this research work, we can conclude that the method and impregnation time influence the acidic properties of boron-modified zirconia. Although the materials

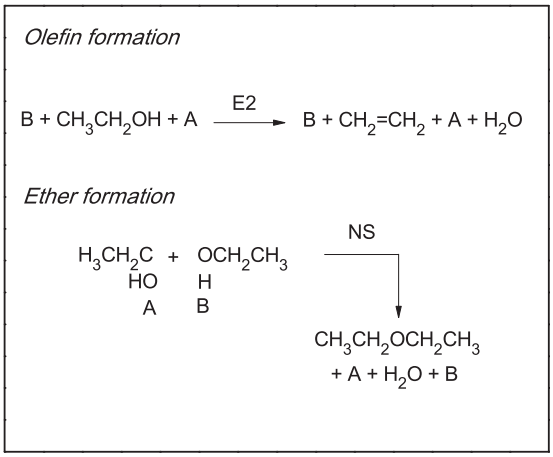

Scheme 1 Ethanol dehydration via elimination reaction (E2) and nucleophilic substitution reaction (NS). A and B represent acidic and basic sites, respectively

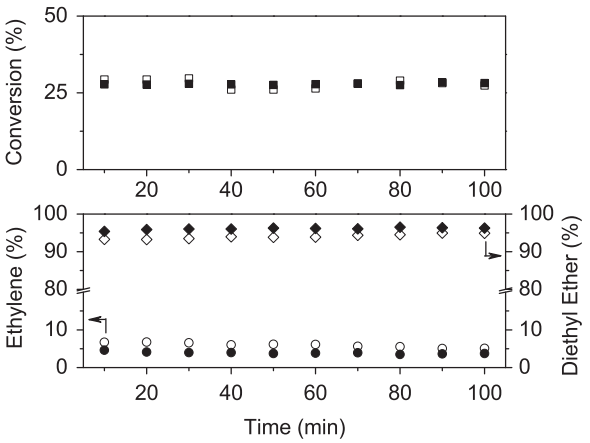

Fig. 15 Ethanol conversion at 250 °C and products distribution using the catalyst ZB1hU: fresh (*open symbol*) and used (*closed symbol*)

showed similarity in several of their properties, in general the boron presence delayed the crystallization process and the solids presented an amorphous tendency. In addition, the specific surface of the modified materials enhanced because the boron incorporation prevented sintering. Nevertheless, beyond the thermal, textural, and structural properties, the method and impregnation time significantly affected the catalytic performance of the solids. Even though all the boron-modified materials showed strong and very strong acid sites, the most active catalysts in the ethanol decomposition were those obtained by the ultrasonic method. Therefore, we can suppose that the catalysts synthesized by ultrasonic impregnation possess more accessible acid sites to the alcohol molecule, which preferably dehydrated to ethylene when the reaction was carried out at 300 °C.

Acknowledgements The authors are grateful to the National Council of Science and Technology (CONACyT) for the Scholarship (227552) granted to María Isabel Arregoitia Quezada, and we also wish to thank the National Technological of Mexico (TecNM) for financial support given during development of this research work (5531.15-P).

Compliance with ethical standards

Conflict of interest The authors declare that they have no conflict of interest.

References

1. Martins RL, Schmal M (2006) Methane activation on superacidic catalysts based on oxoanion modified zirconium oxide. Appl Catal A-Gen 308:143–152
2. Stichert W, Schüth F, Kuba S, Knözinger H (2001) Monoclinic and tetragonal high surface area sulfated zirconias in butane isomerization: CO adsorption and catalytic results. J Catal 198:277–285
3. Sohn JR, Kwon TD, Kim SB (2001) Characterization of zirconium sulfate supported on zirconia and activity for acid catalysis. B Korean Chem Soc 22:1309–1315
4. Vishwanathan V, Balakrishna G, Rajesh B, Jayasri V, Sikhwivhilu LM, Coville NJ (2008) Alkylation of catechol with methanol to give guaiacol over sulphate-modified zirconia solid acid catalysts: The influence of structural modification of zirconia on catalytic performance. Catal Commun 9:2422–2427
5. Yadav GD, Nair JJ (1999) Sulfated zirconia and its modified versions as promising catalysts for industrial processes. Micropor Mesopor Mat 33:1–48
6. Melada S, Ardizzone SA, Bianchi CL (2004) Sulphated zirconia by sol–gel route. The effects of the preparative variables. Micropor Mesopor Mat 73:203–209
7. Cutrufello MG, Diebold U, Gonzalez RD (2005) Optimization of synthesis variables in the preparation of active sulfated zirconia catalysts. Catal Lett 101:5–13
8. Chen WH, Ko HH, Sakthivel A, Huang SJ, Liu SH, Lo AY, Tsai TC, Liu SB (2006) A solid-state NMR, FT-IR and TPD study on acid properties of sulfated and metal-promoted zirconia: Influence of promoter and sulfation treatment. Catal Today 116:111–120
9. Yori JC, Pieck CL, Parera JM (1998) Phosphate as promoter of zirconia for alkane isomerization reactions. Catal Lett 52:227–229
10. Patil PT, Malshe KM, Kumar P, Dongare MK, Kemnitz E (2002) Benzoylation of anisole over borate zirconia solid acid catalyst. Catal Commun 3:411–416
11. D'Souza J, Nagaraju N (2007) Esterification of salicylic acid with methanol/dimethyl carbonate over anion-modified metal oxides. Indian J Chem Techn 14:292–300
12. Xu B-Q, Cheng S-B, Jiang S, Zhu Q-M (1999) Gas phase beckmann rearrangement of cyclohexanone oxime over zirconia-supported boria catalyst. Appl Catal A-Gen 188:361–368
13. Xu B-Q, Cheng S-B, Zhang X, Zhu Q-M (2000) B_2O_3/ZrO_2 for Beckmann rearrangement of cyclohexanone oxime: Optimizing of the catalyst and reaction atmosphere. Catal Today 63:275–282
14. Malshe KM, Patil PT, Umbarkar SB, Dongare MK (2004) Selective *C*-methylation of phenol with metanol over borate zirconia solid catalyst. J Mol Catal A-Chem 212:337–344
15. Madje BR, Patil PT, Shindalkar SS, Benjamin SB, Shingare MS, Dongare MK (2004) Facile transesterification of b-ketoesters under solvent-free condition using borate zirconia solid acid catalyst. Catal Commun 5:353–357
16. Shindalkar SS, Madje BR, Hangarge RV, Patil PT, Dongare MK, Shingare MS (2005) Borate zirconia mediated

Knoevenagel condensation reaction in water. J Korean Chem Soc 49:377–380
17. Shindalkar SS, Madje BR, Shingare MS (2005) Ultrasonically accelerated Knoevenagel condensation reaction at room temperature in distilled water. Indian J Chem 44B:1519–1521
18. Osiglio L, Romanelli G, Blanco M (2010) Alcohol acetylation with acetic acid using borated zirconia as catalyst. J Mol Catal A-Chem 316:52–58
19. Liu H, Zhang S, Zhou Y, Zhang Y, Bai L, Huang L (2011) Effect of ultrasonic irradiation on the catalytic performance of PtSnNa/ZSM-5 catalyst for propane dehydrogenation. Ultrason Sonochem 18:19–22
20. Aboul-Fotouh SMK (2013) Effect of ultrasonic irradiation and/or halogenation on the catalytic performance of γ-Al_2O_3 for methanol dehydration to dimethyl ether. J Fuel Chem Technol 41:1077–1084
21. Soo MT, Prastomo N, Matsuda A, Kawamura G, Muto H, Mohd Noor AF, Lockman Z, Cheong KY (2012) Elaboration and characterization of sol–gel derived ZrO_2 thin films treated with hot water. Appl Surf Sci 258:5250–5258
22. Ivanov VK, Baranchikov AY, Kopitsa GP, Lermontov SA, Yurkova LL, Gubanova NN, Ivanova OS, Lermontov AS, Rumyantseva MN, Vasilyeva LP, Sharp M, Pranzas PK, Tretyakov YD (2013) pH control of the structure, composition, and catalytic activity of sulfated zirconia. J Solid State Chem 198:496–505
23. Chain CY, Quille RA, Pasquevich AF (2010) Ball milling effect on blends M_2O_3-HfO_2. Anales AFA 21:131–134
24. Deqing W (2009) Effects of additives on combustion synthesis of Al_2O_3–TiB_2 ceramic composite. J Eur Ceram Soc 29:1485–1492
25. Zaleska A, Sobczak JW, Grabowska E, Hupka J (2008) Preparation and photocatalytic activity of boron-modified TiO_2 under UV and visible light. Appl Catal B-Environ 78:92–100
26. Mao D, Lu G, Chen Q (2005) Vapor-phase Beckmann rearrangement of cyclohexanone oxime over B_2O_3/TiO_2–ZrO_2: the effect of catalyst calcination temperature and solvent. Appl Catal A-Gen 279:145–153
27. Hernández Enríquez JM, Garcia Serrano LA, García Alamilla R, Cortez Lajas LA, Cueto Hernández A (2009) Síntesis, caracterización y evaluación catalítica de un ZrO_2 con fase monoclínica. Superficies y Vacío 22:1–9
28. Said AE-AA, El-Wahab MMA, El-Aal MA (2014) The catalytic performance of sulfated zirconia in the dehydration of methanol to dimethyl ether. J Mol Catal A-Chem 394:40–47
29. Holly S (1976) In: Szabó ZG, Kalló D (eds) Contact catalysis. Chapter 6. Infrared absorption spectroscopy, Vol. 2. Elsevier, Amsterdam, pp 263–289
30. Gautam C, Yadav AK, Singh AK (2012) A review on infrared spectroscopy of borate glasses with effects of different additives. ISRN Ceram 2012:1–17 doi:10.5402/2012/428497
31. Sinhamahapatra A, Sutradhar N, Ghosh M, Bajaj HC, Panda AB (2011) Mesoporous sulfated zirconia mediated acetalization reactions. Appl Catal A-Gen 402:87–93
32. Sinhamahapatra A, Pal P, Tarafdar A, Bajaj HC, Panda AB (2013) Mesoporous borated zirconia: A solid acid–base bifunctional catalyst. ChemCatChem 5:331–338
33. Cid R, Pecchi G (1985) Potentiometric method for determining the number and relative strength of acid sites in colored catalysis. Appl Catal 14:15–21
34. Pizzio LR (2006) Synthesis and characterization of trifluoromethanesulfonic acid supported on mesoporous titania. Mater Lett 60:3931–3935
35. Bedia J, Rosas JM, Márquez J, Rodríguez-Mirasol J, Cordero T (2009) Preparation and characterization of carbon based acid catalysts for the dehydration of 2-propanol. Carbon 47:286–294
36. Zaki T (2005) Catalytic dehydration of ethanol using transition metal oxide catalysts. J Colloid Interf Sci 284:606–613
37. Ramesh K, Hui LM, Han Y-F, Borgna A (2009) Structure and reactivity of phosphorous modified H-ZSM-5 catalysts for ethanol dehydration. Catal Commun 10:567–571
38. Sheng Q, Ling K, Li Z, Zhao L (2013) Effect of steam treatment on catalytic performance of HZSM-5 catalyst for ethanol dehydration to ethylene. Fuel Process Technol 110:73–78
39. Trakarnpruk W (2013) Dehydration of ethanol over copper and cerium phosphotungstates supported on MCM-41. Mendeleev Commun 23:168–170
40. Jain JR, Pillai CN (1967) Catalytic dehydration of alcohols over alumina: Mechanism of ether formation. J Catal 9:322–330
41. Alharbi W, Brown E, Kozhevnikova EF, Kozhevnikov IV (2014) Dehydration of ethanol over heteropolyacid catalysts in the gas phase. J Catal 319:174–181